

Functional Interactions Between Sae2 and the Mre11 Complex

Hee-Sook Kim,* Sangeetha Vijayakumar,* Mike Reger,[†] Jacob C. Harrison,[‡]
James E. Haber,[‡] Clifford Weil[†] and John H. J. Petrini^{*,§,1}

*Laboratory of Chromosome Biology, Memorial Sloan-Kettering Cancer Center, New York, New York 10021, [‡]Rosenstiel Center and Department of Biology, Brandeis University, Waltham, Massachusetts 02454, [†]Department of Agronomy, Whistler Center for Carbohydrate Research, Purdue University, West Lafayette, Indiana 47907 and [§]Weill Medical College, Cornell University Graduate School of Medical Sciences, New York, New York 10021

Manuscript received August 30, 2007
Accepted for publication December 18, 2007

ABSTRACT

The Mre11 complex functions in double-strand break (DSB) repair, meiotic recombination, and DNA damage checkpoint pathways. Sae2 deficiency has opposing effects on the Mre11 complex. On one hand, it appears to impair Mre11 nuclease function in DNA repair and meiotic DSB processing, and on the other, Sae2 deficiency activates Mre11-complex-dependent DNA-damage-signaling via the Tel1–Mre11 complex (TM) pathway. We demonstrate that *SAE2* overexpression blocks the TM pathway, suggesting that Sae2 antagonizes Mre11-complex checkpoint functions. To understand how Sae2 regulates the Mre11 complex, we screened for *sae2* alleles that behaved as the null with respect to Mre11-complex checkpoint functions, but left nuclease function intact. Phenotypic characterization of these *sae2* alleles suggests that Sae2 functions as a multimer and influences the substrate specificity of the Mre11 nuclease. We show that Sae2 oligomerizes independently of DNA damage and that oligomerization is required for its regulatory influence on the Mre11 nuclease and checkpoint functions.

THE DNA damage response is a highly conserved process that prevents genome instability. In budding yeast, checkpoint signaling is initiated by the yeast ataxia-telangiectasia mutated/ataxia-telangiectasia and Rad3-related (ATM/ATR) homologs, Mec1/Tel1, and is propagated via the effector kinases Chk1 and Rad53 (the Chk2 homolog). DNA damage sites are recognized by two different types of sensors, specific for single-strand DNA (ssDNA) or double-strand breaks (DSBs). RPA (a eukaryotic ssDNA-binding protein) recognizes ssDNA damage sites in cooperation with replication factor C (RFC)-like and PCNA-like (the 9-1-1) complexes. The Mre11 complex consists of three highly conserved members—*MRE11*, *RAD50*, and *XRS2* (*NBS1* in mammals)—and appears to be primarily required for signaling the presence of DSBs (reviewed in ZHOU and ELLEDGE 2000; D'AMOURS and JACKSON 2002; PETRINI and STRACKER 2003; STRACKER *et al.* 2004).

Spo11 catalyzes the formation of DSBs to initiate meiotic recombination. In *rad50S* mutants, Spo11 remains covalently attached at the DSB ends that it forms (KEENEY *et al.* 1997). *Sae2Δ* cells exhibit the same retention of Spo11 at meiotic DSBs, consistent with the view that, in both mutants, Mre11 nuclease function is impaired (KEENEY and KLECKNER 1995; MCKEE and KLECKNER 1997; PRINZ *et al.* 1997). This view is sup-

ported by the fact that Spo11 retention is also seen in nuclease-deficient alleles of *MRE11* (NAIRZ and KLEIN 1997; MOREAU *et al.* 1999).

In vitro, Mre11 has both endo- and exonuclease activity (D'AMOURS and JACKSON 2002). Mutations of conserved histidine residues (*e.g.*, H125N) in the phosphoesterase domain eliminate both activities; however, *in vivo* Mre11-H125N has apparently normal exonuclease activity in degrading an HO-endonuclease-generated DSB (MOREAU *et al.* 2001; LEE *et al.* 2002). These data, and the fact that it is a 3'-5' exonuclease, support the interpretation that the Mre11 complex is not directly involved in the 5'-3' resection of DSB ends. Spo11 removal from meiotic DSBs and DNA hairpin cleavage in mitotic cells, both presumably requiring endonuclease activity, are abrogated by Mre11 nuclease deficiency (LOBACHEV *et al.* 2002; YU *et al.* 2004).

rad50S and *sae2Δ* also affect Mre11 nuclease functions in mitotic cells (RATTRAY *et al.* 2001). Both mutations impair the processing of hairpin DNA structures (LOBACHEV *et al.* 2002; YU *et al.* 2004) and camptothecin (CPT)-induced Top1 cleavage complexes (VANCE and WILSON 2002; DENG *et al.* 2005). These phenotypes are also exhibited by nuclease-deficient *mre11* mutants. In addition, *rad50S* and *sae2Δ* mutants exhibit synthetic lethality with *rad27Δ* (*FEN1* in human), another flap endonuclease that is required for Okazaki fragment maturation (DEBRAUWERE *et al.* 2001; MOREAU *et al.* 2001). It has recently been shown that Sae2 itself possesses endonuclease activity, suggesting the possibility that

¹Corresponding author: Laboratory of Chromosome Biology, MSKCC, 1275 York Ave., RRL 901C, New York, NY 10021.
E-mail: petrini@mskcc.org

Sae2 may play dual roles: as a regulator of Mre11 nuclease function and/or as a nuclease (LENGSFELD *et al.* 2007).

Previously, we demonstrated that both *rad50S* and *sae2Δ* suppress the checkpoint phenotype of Mec1 deficiency via a conserved pathway dependent on the Mre11 complex and Tel1 (referred to as the TM pathway) (USUI *et al.* 2001, 2006; MORALES *et al.* 2005). *sae2Δ* also prevents the normal turning off of the DNA damage checkpoint once a DSB is repaired (CLERICI *et al.* 2006). In contrast, overexpression of *SAE2* suppresses both *MEC1* and *TEL1* kinase activity modifying Rad53 and also prevents the damage-induced phosphorylation of Mre11. These observations suggest that Sae2 may be an inhibitory factor for the Mre11-complex checkpoint function.

Supporting this possibility, we report here that *SAE2* overexpression enhances the methyl methanesulfonate (MMS) sensitivity of *mec1Δ rad50S* cells, suggesting inhibition of the TM pathway. We have isolated *sae2* alleles that fail to enhance this MMS sensitivity and recovered among them *sae2* alleles that alter the Mre11 effect on specific types of substrates. For example, the N terminus of Sae2 appears to be required specifically for the Mre11 nuclease to open hairpin DNA structures, but not for Spo11 cleavage. Further, Sae2 appears to function as an oligomer, and self-interaction is correlated with Sae2 influence on the Mre11 complex's nuclease and checkpoint functions.

MATERIALS AND METHODS

Yeast strains: The following strains are of W303 background (*MATa*, α or α/α *trp1-1 ura3-1 his3-11,15 leu2-3,112 ade2-1 can1-100 RAD5+*, originally from R. Rothstein): JPY2252 (*MATa sae2Δ*), JPY2253 (*MATa FLAG-SAE2*), JPY2254 (*MATa FLAG-sae2-12*), JPY2255 (*MATa FLAG-sae2-58*), JPY2256 (*MATa FLAG-sae2-1*), JPY2258 (*MAT α sae2Δ*), JPY2259 (*MAT α FLAG-SAE2*), JPY2261 (*MAT α FLAG-sae2-1*), JPY2262 (*MAT α FLAG-sae2-12*), JPY2264 (*MAT α FLAG-sae2-58*), JPY2290 (*MAT α FLAG-sae2-51*), JPY2308 (*MAT α /α sae2Δ/sae2Δ*), JPY2309 (*MAT α /α FLAG-SAE2/FLAG-SAE2*), JPY2310 (*MAT α /α FLAG-sae2-1/FLAG-sae2-1*), JPY2311 (*MAT α /α FLAG-sae2-12/FLAG-sae2-12*), JPY2312 (*MAT α /α FLAG-sae2-58/FLAG-sae2-58*), JPY2318 (*MAT α /α sae2Δ/FLAG-sae2-51*), JPY2335 (*MAT α /α rad27Δ/RAD27 sae2Δ/SAE2*), JPY2338 (*MAT α /α rad27Δ/RAD27 FLAG-SAE2::LEU2/SAE2*), JPY2339 (*MAT α /α rad27Δ/RAD27 FLAG-sae2-1::LEU2/SAE2*), JPY2340 (*MAT α /α rad27Δ/RAD27 FLAG-sae2-12::LEU2/SAE2*), JPY2344 (*MAT α /α rad27Δ/RAD27 FLAG-sae2-51::LEU2/SAE2*), JPY2345 (*MAT α /α rad27Δ/RAD27 FLAG-sae2-58::LEU2/SAE2*), JPY2518 (*MATa FLAG-SAE2::LEU2 mec1Δ sml1Δ*), JPY2540 (*MATa FLAG-sae2-1::LEU2 mec1Δ sml1Δ*), JPY2557 (*MATa FLAG-sae2-12::LEU2 mec1Δ sml1Δ*), JPY2589 (*MATa FLAG-sae2-51::LEU2 mec1Δ sml1Δ*), JPY2606 (*MATa FLAG-sae2-58::LEU2 mec1Δ sml1Δ*), JPY2666 (*MATa sae2Δ mec1Δ sml1Δ*), JPY2247 (*MATa SAE2-HA::URA3, YLL1103* from Longhese; BARONI *et al.* 2004), JPY2248 (*MATa SAE2-HA::URA3 mec1Δ sml1Δ, DMP380* from Longhese; BARONI *et al.* 2004). The following strains are of A364a background: JPY319 (*MATa WT*), JPY321 (*MATa mec1-1 sml1*), JPY326 (*MATa rad50S mec1-1 rad53 sml1*), JPY352 (*MATa rad50S mec1-1 sml1*), JPY847 (*MATa rad50S mec1-1 tel1Δ sml1*), JPY848 (*MATa rad50S sae2Δ mec1-1 sml1*), JPY851 (*MATa sae2Δ*).

mec1-1 sml1), JPY3009 (*MATa mec1-1 sml1 FLAG-SAE2*), JPY3010 (*MATa mec1-1 sml1 FLAG-sae2-1*), and JPY3011 (*MATa mec1-1 sml1 FLAG-sae2-12*). The following strains are of SK1 background: JPY839 (*MATa rad50S sae2Δ TRP1*) and JPY840 (*MATa sae2*). The following strains were used for chromatin immunoprecipitation: JPY1475 (*MATa WT hoΔ hmlΔ::ADE1 hmrΔ::ADE1 ade1 leu2-3,112 lys5 trp1::hisG ura3-52 ade3::GAL::HO bar1::ADE3::bar1*, H1072 from Lichten; SHROFF *et al.* 2004) and JPY2319 (*MATa sae2Δ*).

Construction of yeast strains: Yeast strains carrying the *SAE2* or *RAD27* deletion were obtained by PCR disruptions using pFA vectors containing *KAN* (G418 resistant), *HYG* (hygromycin resistant), or *TRP1* markers. For the integration of *sae2* mutants, the *SAE2* open reading frame (ORF) was swapped with either a *KAN* or a *HYG* marker and *FLAG-SAE2* or *FLAG-sae2* mutants were integrated at this locus. Deletions and integrations of these genes were verified by PCR. All primers and plasmids used for the mutant constructions and genotyping are available upon request.

***sae2* mutant screen:** JPY352 (*rad50S mec1*) strains were cotransformed with PCR random-mutagenized *FLAG-sae2* fragments and pRS425 vector digested with *SacII* and *KpnI*. Transformants were replica plated on media containing 0.007% MMS. *rad50S mec1* transformed with empty vector and *FLAG-SAE2/2μ* were used as controls. The *sae2* mutants were screened for the inability to increase MMS sensitivity of *rad50S mec1* cells. Approximately 20,000 colonies were screened for this phenotype. To eliminate the mutants that do not express Flag-sae2 proteins, trichloroacetic acid (TCA)-extracted whole proteins were prepared and expression of *sae2* mutants was analyzed by Western blot using a monoclonal Flag-antibody. *FLAG-sae2* mutant plasmids were then rescued from these cells. The MMS sensitivity and protein expression of these clones were reverified. A total of 15 *sae2* mutants were isolated and sequenced. To compensate for the bias in screening, due to the N-terminal tagging of Sae2, Sae2 was tagged at the C terminus with HA. Three N-terminal truncation alleles, *sae2-82*, *sae2-139*, and *sae2-146*, were isolated by the C-terminal HA tagging. These were N-terminal 120-amino-acid truncation mutants (referred to as a *sae2-ΔN₁₂₀*). In addition, two N-terminal truncations, *sae2-ΔN₁₇₀* and *ΔN₂₂₅*, were also generated.

Analysis of MMS, UV, and CPT sensitivity: Fresh growing cells were serially diluted and spotted onto solid media containing different concentrations of indicated drugs or irradiated with indicated UV doses. Plates were photographed after 3 days of incubation at 30°. For the transient treatment, exponentially growing cells were untreated or treated with the indicated concentrations of drugs and the same number of cells was spotted onto a YPD plate. The percentage of viability was determined by counting colonies after 3 days of incubation.

Immunoprecipitation and Western blot analysis: About 5×10^8 cells were lysed in lysis buffer [25 mM Tris-HCl (pH 7.5), 1 mM EDTA, 0.5% NP-40, 10% glycerol, 1 mM phenylmethylsulfonyl fluoride, 1 mM dithiothreitol, 1 × complete and 150 mM NaCl] using FASTprep (Q-BIOgene). Extracts were immunoprecipitated with HA or Flag antibody. Coprecipitated proteins were analyzed by Western blot.

Chromatin immunoprecipitation and real-time PCR: Cell extracts were prepared as described (SHROFF *et al.* 2004) and immunoprecipitated with anti-Mre11 serum. The precipitated DNA was quantitated by real-time PCR using the 7900HT (Applied Biosystems, Foster City, CA) and Light Cycler 480 sequence detection system (Roche). Amplified double-stranded DNA product during 40 cycles was detected by SYBR Green I. All measurement of PCR product was quadruplicated and compared with 1000-fold linear range standard DNA controls prepared from the wild-type strain. Efficiency of Mre11

association with a HO break, 0.05 and 66 kb from the break, was obtained by normalizing the chromatin-immunoprecipitated DNA to input DNA. The sequences of primers used for the real-time PCR are available upon request.

Checkpoint, adaptation, and recovery assays: For G₂/M checkpoint assays, cells were arrested in G₁ with α -factor and released into 0.02% or 0.03% MMS. Cells were collected at the indicated time points and stained with DAPI. The percentage of nuclear division was assessed as described (USUI *et al.* 2001).

YMV80 *sae2* Δ cells transformed with the *sae2* plasmids (CEN) were assayed for repair and recovery after a single HO-DSB induction. To assay G₂/M arrest and recovery, cells were grown overnight either in YEP-lactate media or in synthetic media plus raffinose at 30°. Galactose was added to the liquid culture to a final concentration of 2% and the culture was incubated at 30° for a further 6 hr. Cells were then spread onto YEP-galactose plates and incubated at 30° overnight. At 24 hr the plates were examined for the percentage of cells that were still arrested as G₂/M dumbbells, as an indication of failed repair or delayed recovery. In parallel, samples were plated directly from preinduction media onto YEPD and YEP-galactose plates to determine the percentage of viability.

Telomere Southern blot: *Xho*I-digested genomic DNA was analyzed for telomere length by Southern blot hybridizing ³²P-labeled telomere oligo probes.

Analysis of meiotic DSB processing: Following 4.5 and 9 hr in sporulation media, *Eco*RI-digested genomic DNA was assayed for meiotic DSB processing at the *THR4* locus by Southern blot.

RESULTS

Sae2 blocks the TM pathway: We showed previously that Sae2 deficiency suppresses the MMS sensitivity of *mec1* mutants (USUI *et al.* 2001) through the TM pathway, which suggests that Sae2 may antagonize Mre11-complex checkpoint or DNA repair functions. This view predicts that *SAE2* overexpression would increase the sensitivity of *mec1* and *rad50S mec1* cells to genotoxic stress. To test this idea, Flag-epitope-tagged *SAE2* in a high-copy (2 μ) or in a low-copy (CEN) plasmid was introduced into *sae2* Δ strains that were otherwise wild type, *rad50S*, *mec1*, or *rad50S mec1*. High-copy plasmid produced at least five times more Flag-Sae2 proteins compared to *SAE2*/CEN (Figure 1B). *SAE2* overexpression increased sensitivity to UV-induced damage (Figure 1A) in *mec1* and *rad50S mec1* cells, whereas it did not affect wild type or *rad50S*. Serially diluted cells carrying *SAE2* plasmids were transferred onto solid media containing MMS, and *SAE2* overexpression again showed increased MMS sensitivity only in the absence of *mec1* (Figure 1C)

The effect of *SAE2* overexpression on *mec1* and *rad50S mec1* cells reflected an effect on the TM pathway. *SAE2* overexpression was carried out in *rad50S mec1 rad53* Δ and *rad50S mec1 tel1* Δ mutants; both Rad53 and Tel1 deficiency block the TM pathway (USUI *et al.* 2001). *SAE2* overexpression did not further increase the MMS sensitivity of *rad50S mec1* cells lacking either *RAD53* or

TEL1 (Figure 1, C and D). The effect of *SAE2* overexpression on the G₂/M checkpoint was assessed by releasing G₁-arrested cells into 0.02% MMS and scoring nuclear division by counting binucleated cells (Figure 1E). Wild-type cells were arrested in G₂/M, whereas binucleated cells accumulated in *mec1* cells. The *mec1* arrest defect was suppressed by *rad50S* as shown previously; however, in *rad50S mec1* cells overexpressing *SAE2*, binucleated cells were again increased, similar to the *mec1* mutant. These data argue that *SAE2* overexpression impairs the TM pathway, supporting the interpretation that Sae2 and the Mre11 complex functionally interact.

Both the Mre11 complex and Tel1 influence telomere maintenance (RITCHIE and PETES 2000; D'AMOURS and JACKSON 2002; LUNDBLAD 2002; PANDITA 2002; D'ADDA DI FAGAGNA *et al.* 2003). *sae2* Δ cells exhibited slightly elongated telomeres and caused further telomere elongation in combination with a *mec1* mutation, similar to observations of *rad50S* cells (KIRONMAI and MUNIYAPPA 1997; data not shown). This telomere lengthening was dependent on *TEL1*, again suggesting a dependence on the TM pathway (data not shown). Thus, we examined whether *SAE2* overexpression inhibited telomere lengthening, but found that *SAE2* overexpression did not affect telomere length, regardless of the genotypes (Figure 1F). UV sensitivity of *mec1 rad50S* cells was not affected by extremely shortened or elongated telomeres caused by *tlc1* Δ , a RNA component of the telomerase complex, or by *rif1* Δ , a negative regulator of telomerase (data not shown). These data suggest that controlling telomere length is not a primary target of Sae2 in regulation of the TM pathway.

Sae2 influences DNA repair events that require the Mre11 nuclease: To gain mechanistic insight regarding the functional interaction between Sae2 and the Mre11 complex, we mutagenized *SAE2* and screened for alleles that failed to sensitize *rad50S mec1* cells to MMS. Approximately 20,000 colonies of *rad50S mec1* strains transformed with randomly mutagenized *FLAG-sae2* fragments were tested on solid media containing 0.007% MMS. Fifteen alleles were isolated (Figure 2C). *sae2-13*, *-19*, and *-20* appeared to encode unstable *sae2* proteins and behaved similarly to the empty vector control. These mutations are clustered between amino acids (aa) 195–198 (Figure 2C), indicating that this region is important for protein stability. Unexpectedly, overexpression of *sae2-33* or *sae2-105* further sensitized *rad50S mec1* to MMS compared to wild-type *SAE2* overexpression.

sae2 Δ phenocopies Mre11 nuclease deficiency in the repair of CPT-induced DNA damage, the metabolism of DNA hairpins, the processing of meiotic DSBs, and synergism with *rad27* Δ (CAO *et al.* 1990; KEENEY and KLECKNER 1995; NAIRZ and KLEIN 1997; PRINZ *et al.* 1997; DEBRAUWERE *et al.* 2001; MOREAU *et al.* 2001; LOBACHEV *et al.* 2002; VANCE and WILSON 2002; YU *et al.* 2004; DENG *et al.* 2005). As each of these contexts are

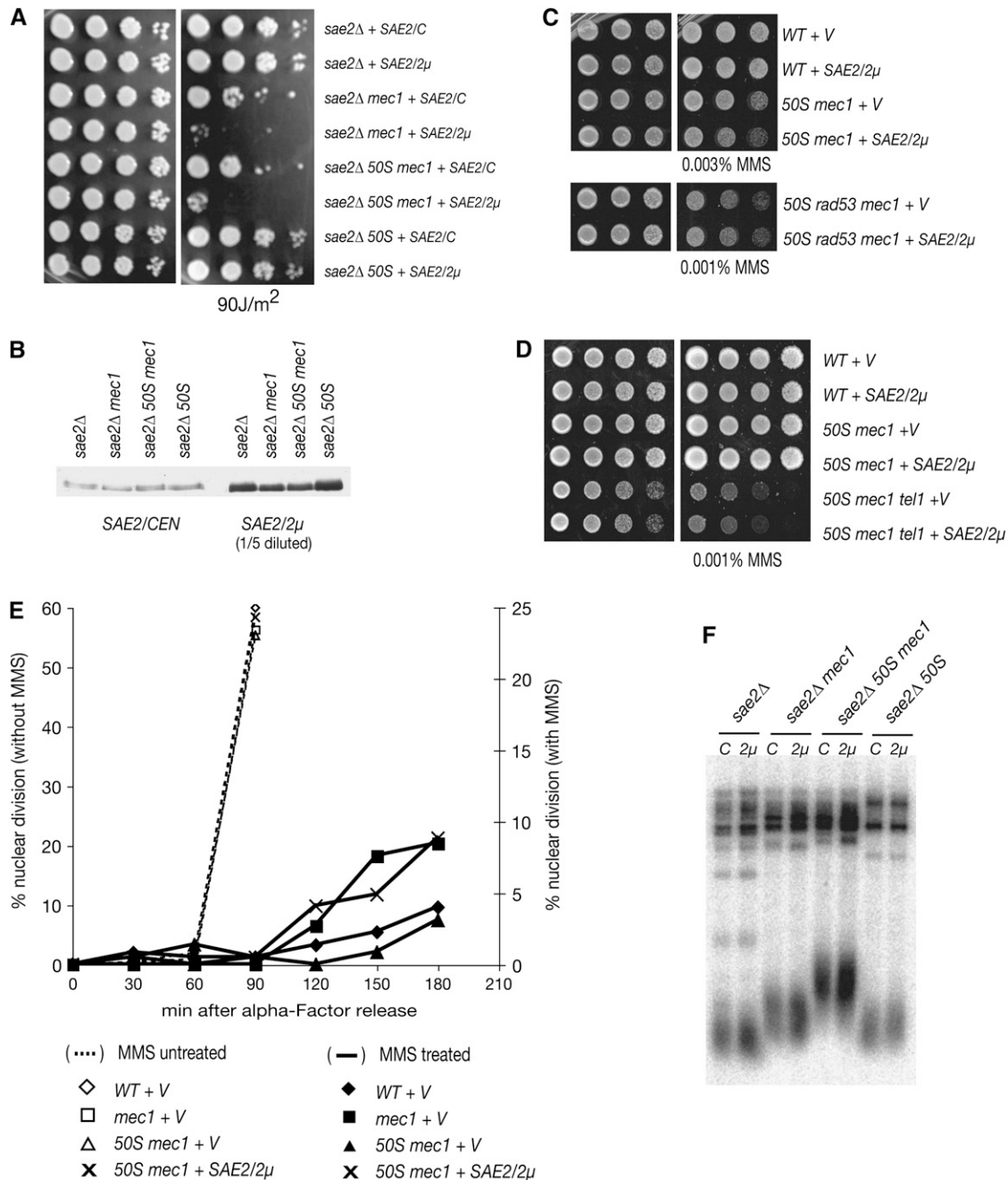


FIGURE 1.—Sae2 blocks the TM pathway. (A) *SAE2* overexpression increases the UV sensitivity of *mec1* and *rad50S mec1*. Yeast strains carrying *FLAG-SAE2/CEN* (low copy) or *FLAG-SAE2/2μ* (high copy) were 1/10 serially diluted, spotted onto plates, and left untreated (left) or irradiated with UV (right). (B) Whole-cell extracts were prepared from the strains listed in A by TCA precipitation and were Western blotted with anti-Flag antibody. Extracts from high-copy transformants were diluted to 1/5. (C and D) *SAE2* overexpression influences *TEL1*- and *RAD53*-dependent pathways. MMS sensitivity of *rad50S mec1 tel1* or *rad50S mec1 rad53* cells carrying empty vector or *FLAG-SAE2/2μ* was determined by spotting experiments (1/5 serial dilution). (E) *SAE2* overexpression blocks G₂/M checkpoint. G₁-arrested cells were released into 0.02% MMS and the percentage of binucleated cells was determined. Solid symbols with straight lines indicate MMS-treated samples; wild type with 2μ vector (◆), *mec1* with 2μ (■), *rad50S mec1* with 2μ (▲), and *rad50S mec1* with *SAE2/2μ* (×). Open symbols with dashed lines indicate MMS-untreated samples. (F) Telomere length control is not a primary target of Sae2 in regulation of the TM pathway. The strains with either *SAE2/CEN* or *SAE2/2μ* were analyzed for telomere length by Southern blot.

likely to require the metabolism of distinct DNA lesions, we asked whether any of the *sae2* alleles obtained were separation-of-function mutants that affected some Mre11-dependent processes while leaving others intact.

sae2 alleles were integrated at the *SAE2* locus and analyzed as described below. The data obtained are summarized in Table 1. *sae2-12* and *sae2-58* strains exhibited MMS and CPT sensitivity comparable to

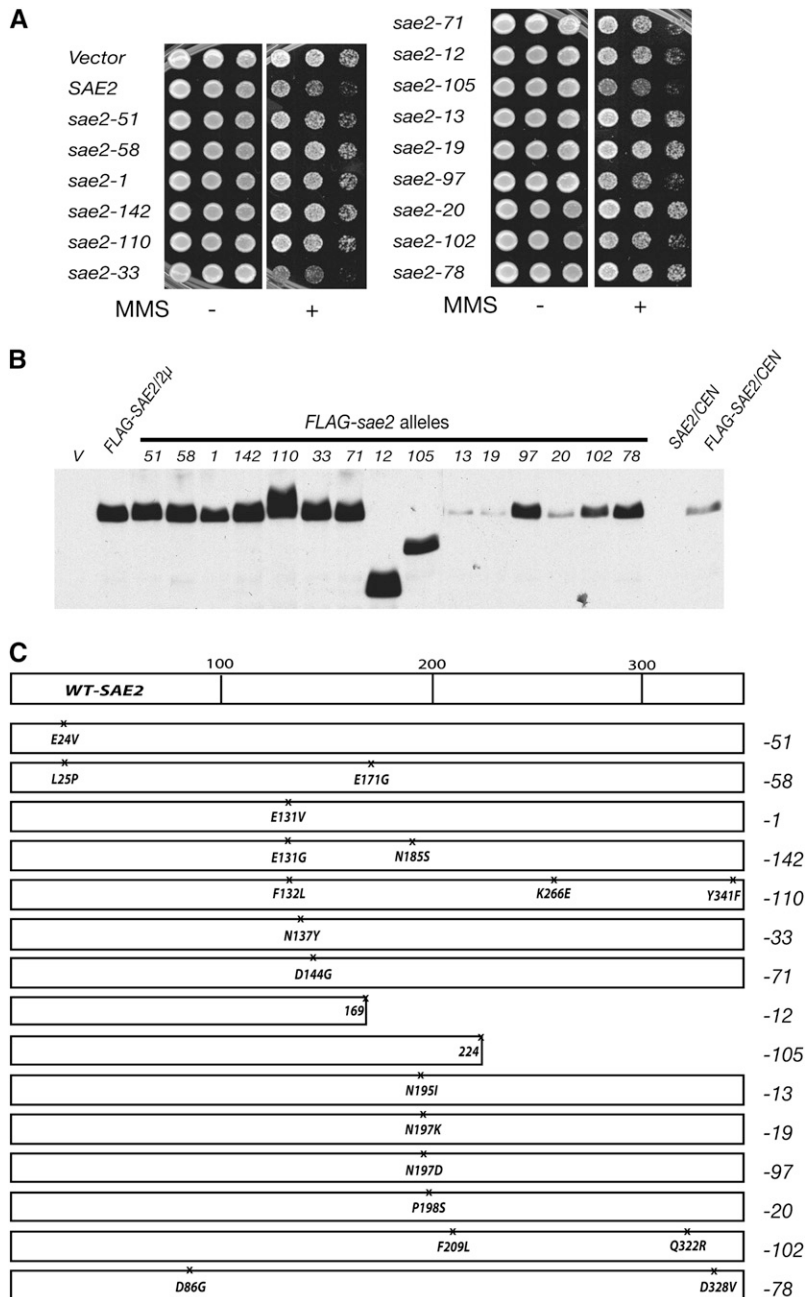


FIGURE 2.—Isolation of *sae2* alleles that fail to sensitize *rad50 Δ mec1* to MMS. (A) *rad50 Δ mec1* (JPY352) cells carrying *sae2* mutants isolated from the screen were reverified for the MMS sensitivity by spotting experiments (1/5 serial dilution, 0.006% MMS). (B) Protein expression level of *sae2* mutants. The TCA-extracted whole proteins were prepared from *sae2 Δ mec1* (JPY851) carrying *sae2* mutant plasmid (2 μ) and Western blotted with anti-Flag antibody. (C) Schematic of *sae2* alleles and the location of mutation sites.





sae2 Δ , whereas *sae2-1* and *sae2-51* were indistinguishable from wild type in this regard (Figure 3A). Accordingly, *sae2-12* and *-58* behaved as *sae2 Δ* and suppressed the MMS sensitivity of *mec1 Δ* (Figure 3B). Although *sae2-1* did not exhibit MMS or CPT sensitivity (Figure 3A), as with *sae2-12* and *sae2-58*, this allele behaved as a hypomorphic mutation with respect to the suppression of *mec1 Δ* MMS sensitivity. As expected, *sae2-51* behaved as wild type and did not affect the MMS sensitivity of *mec1 Δ* .

sae2 Δ did not suppress the *mec1* growth defect in response to CPT, in contrast to MMS treatment (Figure 3B). However, a *sae2-1 mec1 Δ* double mutant grew about five times better than *mec1 Δ* or *sae2 Δ mec1 Δ* strains on a CPT-containing plate. These data indicate that Mec1

influences the regulation of Mre11-complex nuclease function by Sae2.

To examine whether the *sae2* mutants were proficient in Spo11 removal from meiotic DSBs, diploid W303 cells homozygous for each of the *sae2* alleles were examined for DSB processing (Figure 3C). Genomic DNA prepared from the *sae2* mutant cells at 4.5 and 9 hr after meiosis induction was examined for accumulation of unprocessed DSBs at the *THR4* meiotic hotspot by Southern blot. Unprocessed DSBs in *sae2 Δ* cells were detected as a discrete 5.7-kb fragment band (Figure 3C). The unprocessed DSBs in *sae2 Δ* , *sae2-12*, and *sae2-58* homozygotes were two to three times more abundant than in wild type at 4.5 and 9 hr, while *sae2-1* was similar

TABLE 1
Summary of mutant *sae2* phenotypes

Lesion:	Complex substrate					Spo11	
<i>sae2</i> allele	Growth on MMS	Growth on CPT	With <i>rad27Δ</i>	Hairpin processing (Ade ⁺ revertants/10 ⁷) ^a	Sporulation efficiency: % tetrads	% viable spores	Recovery ^b
<i>SAE2</i>	+	+	Viable	37.0 ± 6.1	68.3	100	+
<i>sae2-1</i>	+	+	Viable	41.5 ± 10.6	70.9	93.8	+
<i>sae2-51</i>	+	+	Viable	1.7 ± 1.5	49.0 ^c	93.0 ^d	ND
<i>sae2-58</i>	–	–	Lethal	8.3 ± 9.1	12.3	22.5	–
<i>sae2-12</i>	–	–	Lethal	2.0 ± 1.7	0.3	ND	–
<i>sae2Δ</i>	–	–	Lethal	0	0	ND	–

Integrated *sae2* mutations were examined (+, wild-type phenotype; –, null phenotype). Synthetic lethality with *rad27Δ* was determined by tetrad dissection of diploids heterozygous for *sae2* and *rad27Δ*. Sporulation efficiency of *sae2* diploids was examined. The percentage of tetrads was determined by counting tetrads 48 hr after induction of meiosis.

^a *sae2Δ* cells carrying *sae2* mutant plasmids were analyzed for the ability to repair hairpin DNA structure, and experiments were performed as described (WEIL and KUNZE 2000). Repair efficiency is measured by the frequency of Ade⁺ revertants.

^b Recovery phenotype was assessed in YMV80 background as described (VAZE *et al.* 2002). YMV80 *sae2Δ* cells were transformed with *sae2* mutant plasmid (pRS314/CEN) and the percentage of viability was determined in response to a HO break. ND, not determined.

^c In a separate experiment, 49% of *sae2-51/sae2Δ* cells sporulated after 21 hr of sporulation induction, comparable to wild type (52% sporulation).

^d *sae2-51/sae2Δ* diploid was used.

to wild type. Since unprocessed DSBs block spore formation, we also tested sporulation efficiency in the *sae2* mutants. The trend observed in DSB accumulation was recapitulated in spore viability. *sae2-1* cells (70.9%) sporulated and 93.8% of the spores were viable, comparable to wild type. In contrast, only 12.3 and 0.3% of cells formed tetrads in *sae2-58* and *sae2-12* diploids (Figure 3D and Table 1).

The Mre11 nuclease and Sae2 are required to open DNA hairpin structures (LOBACHEV *et al.* 2002; YU *et al.* 2004). To examine the ability of the *sae2* mutants to process hairpin structures, we took advantage of a transposition assay system in budding yeast. In this assay strain (WEIL and KUNZE 2000), a maize *Ds* transposon is inserted in the middle of the *ADE2* ORF. Expression of the maize *Ac* transposase excises the *Ds* element and leaves a hairpin at the ends of the adjacent chromosomal DNA. These hairpins have to open to be repaired by DSB repair pathways. Repair efficiency can be estimated by the frequency of Ade⁺ revertants. *sae2Δ* strains carrying *sae2* mutant plasmids (2 μ) were examined for the frequency of Ade⁺ revertants (Table 1 and supplemental Table S1 at <http://www.genetics.org/supplemental/>). *SAE2* gave ~37.0 revertants/10⁷ cells whereas *sae2-12*, *sae2-58*, or empty vector transformants gave 2.0, 8.3, or 0 revertants, respectively. *sae2-1* (41.5/10⁷) was similar to wild type. Although *sae2-51* behaved as wild type with respect to checkpoint regulation and to MMS and CPT sensitivity as well as meiotic progression (Table 1; supplemental Table S1 and Figure S2 at <http://www.genetics.org/supplemental/>), this allele exhibited a severe hairpin repair defect (1.7/10⁷). *sae2-51* contains

a *E24V* mutation, indicating that the N-terminal end of Sae2 may be specifically required for the Mre11 nuclease to open hairpin DNA. We note that another N-terminal mutant, *sae2-58*, also cannot process hairpin ends.

Mutations that impair Mre11 nuclease function *in vivo*, such as *sae2Δ* and *mre11-H125N*, are synthetically lethal with Rad27 deficiency (DEBRAUWERE *et al.* 2001; MOREAU *et al.* 2001). Synthetic lethality between *rad27Δ* and *sae2* mutants was analyzed by tetrad dissection. *sae2-12* and *sae2-58* were each lethal with *rad27Δ*, but *sae2-1 rad27Δ* and *sae2-51 rad27Δ* double mutants were viable (Table 1).

Role of Sae2 in checkpoint activation and inactivation: Upon MMS treatment, wild-type cells arrest in G₂/M, whereas checkpoint-deficient *mec1* mutants fail to arrest and undergo nuclear division accompanied by loss of viability. We showed that *sae2Δ* suppresses the checkpoint defects associated with Mec1 deficiency (USUI *et al.* 2001). Integrated *sae2-1*, *sae2-12*, and *sae2-58* were assayed for the rescue of the G₂/M checkpoint defect of *mec1* cells. G₁-arrested cells were released into MMS and binucleated cells were counted every 30 min. As shown in Figure 4A, wild-type cells were arrested in G₂/M while binucleated cells accumulated over time in *mec1* mutants. Approximately 25–29% of *mec1* cells underwent mitosis at 150 min after MMS treatment. This *mec1* defect was rescued in *sae2-12* (Figure 4A, a) or *sae2-58* (Figure 4A, b), indicating that these two alleles behaved as *sae2Δ* and thus were able to rescue the *mec1* checkpoint defect. On the other hand, ~16% of *sae2-1 mec1* cells were similar to *mec1* and went through mitosis 120 and 150 min after MMS treatment (Figure 4A, a). Hence,

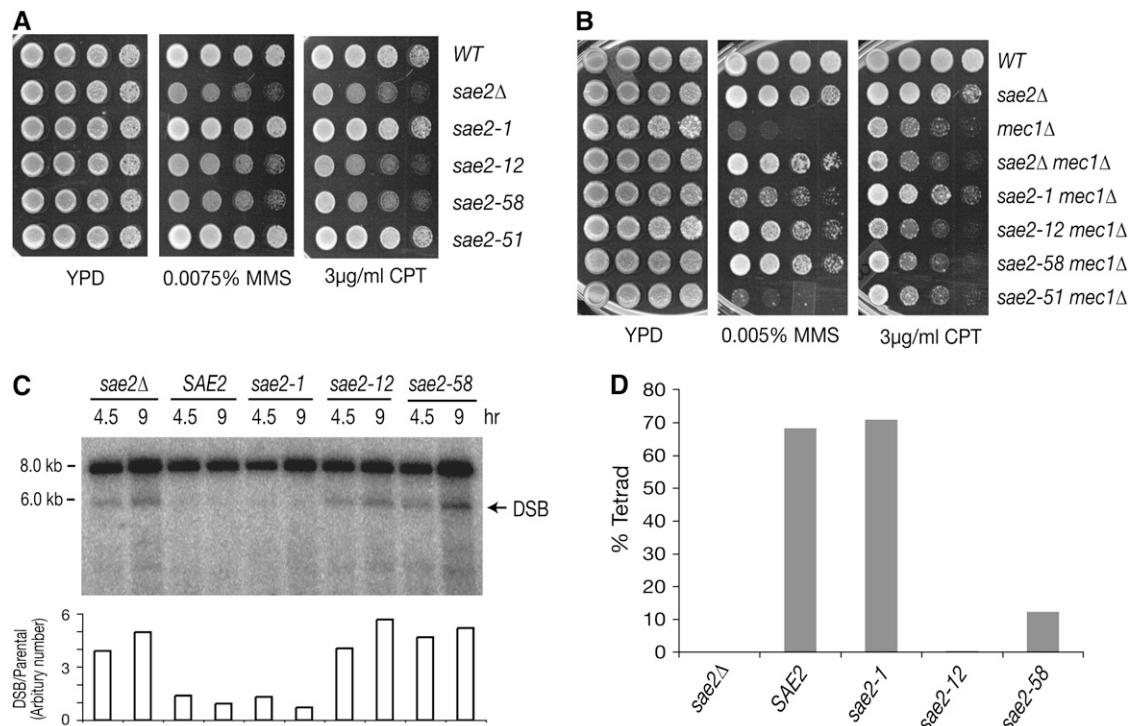


FIGURE 3.—Sae2 influences DNA repair events that require the Mre11 nuclease activity. Integrated *sae2* alleles were examined for their phenotypes. (A) MMS and CPT sensitivity of *sae2* single mutants (1/5 serial dilution). (B) MMS and CPT sensitivity of *sae2* mutants in the absence of *MEC1* (1/5 serial dilution). (C) The ability to remove Spo11-DNA intermediates. Accumulation of unprocessed DSBs in *sae2* mutant diploids was determined by Southern blot. Cells were collected at 4.5 and 9 hr after meiosis induction. *EcoRI*-digested genomic DNA prepared from these cells was examined for accumulation of unprocessed DSB at the *THR4* locus by Southern blot. The unprocessed DSBs were detected as a discrete 5.7-kb fragment band. (D) Sporulation efficiency. Cells were collected at 48 hr after meiosis induction and stained with DAPI. The percentage of tetrads was plotted.

as in other determinations, this allele's behavior is similar to wild type with respect to TM pathway regulation.

When DNA damage is repaired, cells must inactivate checkpoint pathways to resume the cell cycle; this is defined as recovery from checkpoint arrest (LEE *et al.* 1998; PELLICOLI *et al.* 2001; VAZE *et al.* 2002; LEROY *et al.* 2003). It has recently been shown that *sae2Δ* cells are defective for recovery from arrest induced by a long-lived HO-endonuclease-mediated DNA break (CLERICI *et al.* 2006). Accordingly, we examined the panel of *sae2* mutants for their ability to recover from checkpoint arrest. In strain YMV80, DSBs induced by HO endonuclease are repaired by single-strand annealing (SSA) ~6 hr after HO induction (VAZE *et al.* 2002). The DNA damage checkpoint is fully activated in 2 hr after the HO-DSB formation but is turned off for cells to resume cell cycle progression when SSA is completed. YMV80 *sae2Δ* cells were transformed with the *sae2* plasmids (CEN) and then assayed for recovery after HO induction by determining the percentage of cells with dumb-bell shape, indicative of cells that are permanently arrested in G₂. *sae2Δ* cells carrying a *SAE2* plasmid maintained 88% viability (Figure 4B) and only 8.3% cells were still arrested in G₂ at 24 hr after HO induction (Figure 4C). In contrast, the *sae2Δ* cells showed 18.7% viability and 43.8% cells arrested in G₂, consistent with

previous findings (CLERICI *et al.* 2006). *sae2-1* was proficient in recovery similar to wild type (55.8% viability, 15.1% arrest), and *sae2-12* and *sae2-58* behaved as null mutants.

In contrast to results reported by CLERICI *et al.* (2006), the recovery defect of *sae2Δ* was rescued by *tel1Δ*. Recovery was also rescued by C-terminal mutation of Xrs2 that fails to associate the Mre11 complex with Tel1, *xrs2-664* (SHIMA *et al.* 2005). Finally, the recovery defect of *sae2Δ* was suppressed by *PTC2* overexpression (a regulator subunit of phosphatase) and *mec1Δ*, both of which prevent maintenance of Rad53 phosphorylation (Figure 4C). However, the viability was not significantly suppressed by these mutations or *PTC2* overexpression (Figure 4B). These data indicate that compromising the checkpoint or the untimely turning off of it can rescue DNA damage arrest without fully complementing the viability.

Influence of Sae2 on Mre11-DSB association: Physical association of the Mre11 complex with DSBs is vital for its function in checkpoint activation as well as in meiosis (USUI *et al.* 2001; PETRINI and STRACKER 2003; BORDE *et al.* 2004; LISBY *et al.* 2004; SHROFF *et al.* 2004). Therefore, we hypothesized that the inhibition of the TM pathway by *SAE2* overexpression limits Mre11 association with DSBs. Indirect evidence for this possibility

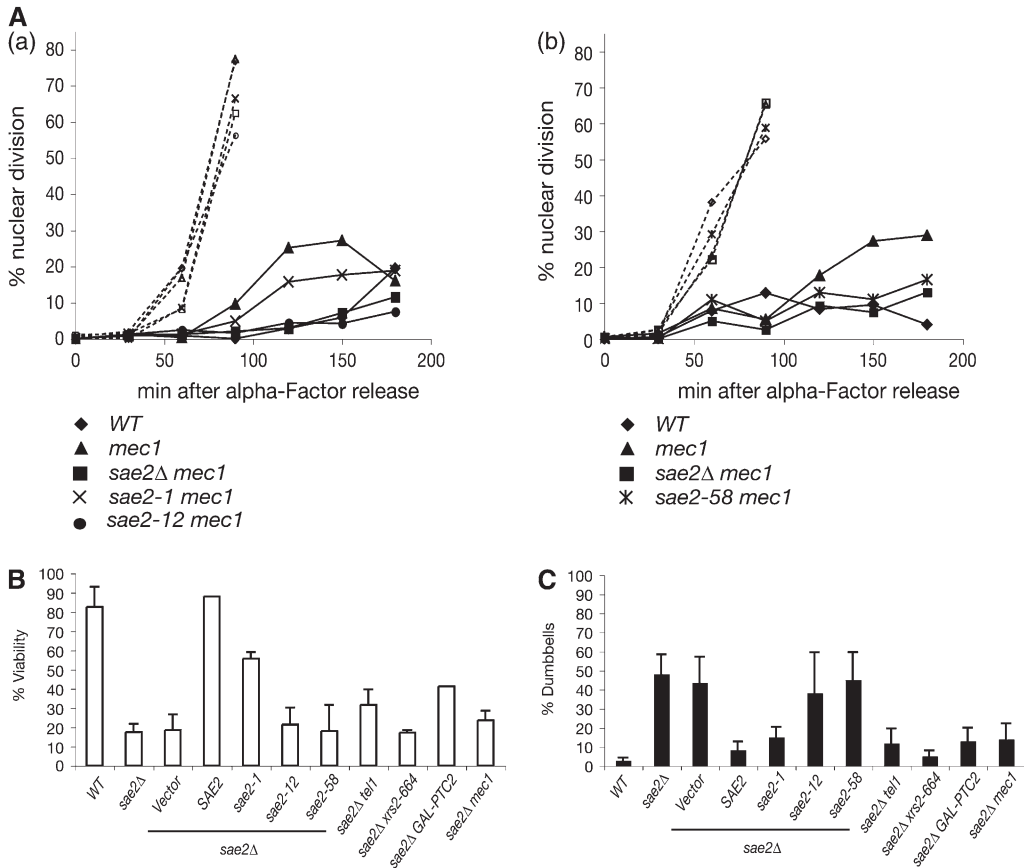


FIGURE 4.—Role of Sae2 in checkpoint activation and inactivation. (A) The rescue of the G₂/M checkpoint defect of *mec1*. G₁-arrested cells were released into 0.02% (a) or 0.03% (b) MMS and the percentage of nuclear division was analyzed by counting binucleated cells. Open symbols with dashed lines indicate MMS-untreated samples. Closed symbols with straight lines indicate MMS-treated samples. Wild type (◆), *mec1* (▲), *sae2Δ mec1* (■), *sae2-1 mec1* (×), *sae2-12 mec1* (●), and *sae2-58 mec1* (✱). (B and C) Recovery and viability in response to an HO break. The percentage of viability (B) and of G₂-arrested cells (C) were determined in YMV80 *sae2Δ* cells carrying *SAE2* or *sae2* mutant plasmids (CEN) and in *sae2Δ tel1*, *sae2Δ xrs2-664*, *sae2Δ GAL-PTC2*, and *sae2Δ mec1* mutant cells.

comes from the apparent requirement for Sae2 in the formation of Mre11 “repair” foci (LISBY *et al.* 2004; CLERICI *et al.* 2006). To test this hypothesis, we carried out chromatin immunoprecipitation (ChIP) experiments to assess Mre11-complex association at an HO break in a *hmrΔ hmlΔ* strain to prevent repair by gene conversion (SHROFF *et al.* 2004). Wild-type and *sae2Δ* cell extracts were immunoprecipitated with anti-Mre11 serum, and Mre11 association at 0.05 kb from the HO break was determined by quantitative PCR. As previously reported (LISBY *et al.* 2004; CLERICI *et al.* 2006), Mre11 associated with a HO break two to three times more efficiently in *sae2Δ* cells, compared to wild type, although Sae2 deficiency did not change the association and dissociation kinetics (Figure 5). Overexpression did not affect Mre11 association (supplemental Figure S5 at <http://www.genetics.org/supplemental/>). These data suggest that regulation of Mre11–DSB association is not the basis of Sae2’s influence on Mre11-complex-mediated checkpoint functions.

Sae2 self-interaction via two domains is critical for its cellular functions: Sae2–Sae2 interaction was observed in a global analysis of two-hybrid interactions (ITO *et al.* 2001). To determine whether the phenotypes of our *sae2* mutant panel could be associated with compromised self-association, we constructed diploid strains carrying integrated *FLAG-SAE2* and *SAE2-HA* and examined their interaction by co-immunoprecipitation

(co-IP) experiments. Cells were either untreated or treated with 0.03% MMS for 2 hr and extracts were immunoprecipitated with anti-HA or anti-Flag antibody. As shown in Figure 6A, Flag-Sae2 coprecipitated with Sae2-HA, and Sae2-HA also coprecipitated with Flag-Sae2 (lanes 5 and 6) regardless of MMS treatment, indicating that Sae2 interacts with Sae2 independently of DNA damage.

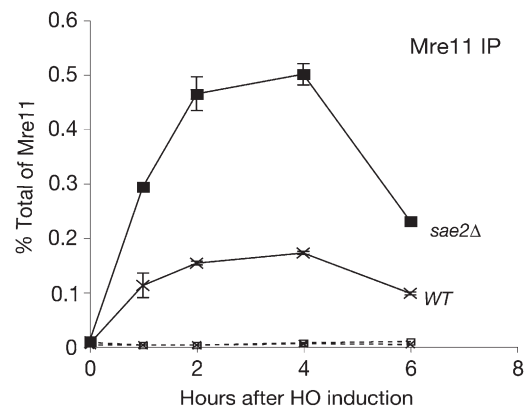


FIGURE 5.—Influence of Sae2 on Mre11–DSB association. Absence of Sae2 increases Mre11 association with DSB. Efficiency of Mre11–DSB association was determined by ChIP and real-time PCR. Mre11 association at 0.05 kb from the break in wild type (×) and in *sae2Δ* (■). The dashed lines indicate Mre11 association at the 66-kb site.

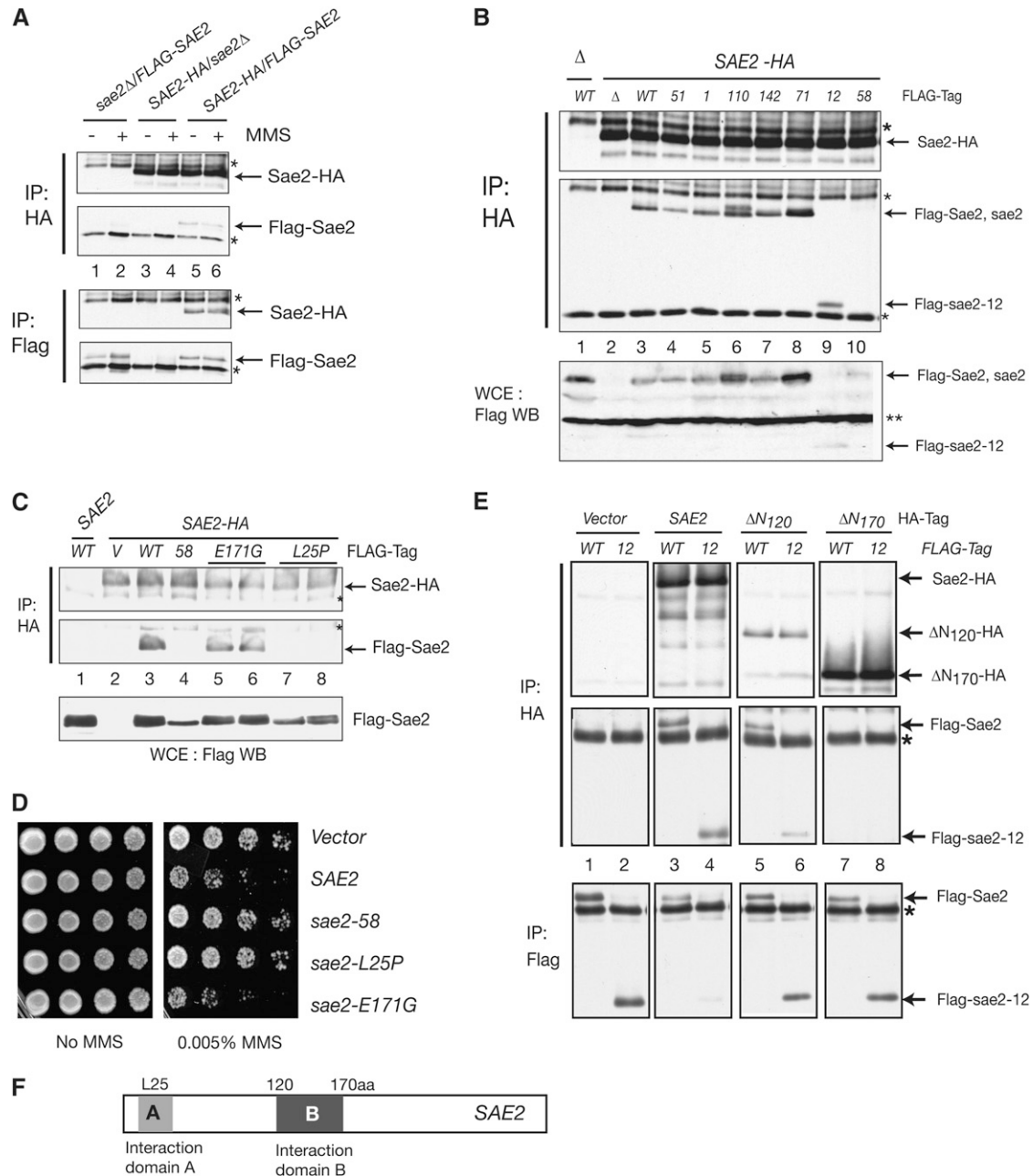


FIGURE 6.—Sae2 self-interaction via two domains is critical for its cellular functions. (A) Sae2 self-interacts regardless of DNA damage. Interaction between Sae2-HA and Flag-Sae2 was examined in diploid strains carrying integrated *SAE2-HA* and *FLAG-SAE2* by co-IP and Western blot. Cells were either untreated or treated with 0.03% MMS for 2 hr. (B) Sae2 self-interaction is required for its cellular functions. The interaction was examined in diploid strains carrying integrated *SAE2-HA* and *FLAG-sae2* mutants by co-IP and Western blot. (C) Residue L25 is required for the Sae2 self-interaction. The interaction was examined in *SAE2-HA* strains carrying Flag-*sae2* mutant plasmids (2 μ). Two independent clones were analyzed for *sae2-E171G* and *sae2-L25P* mutants. (D) Residue L25 is required for the inhibition of the TM pathway. *rad50S mec1* cells were transformed with either *sae2-L25P* or *sae2-E171G* and examined for MMS sensitivity (1/5 dilution). (E) The additional region between 120 and 170 aa is required for the Sae2 interaction. The interaction was examined in *FLAG-SAE2* or *FLAG-sae2-12* strains carrying the N-terminal truncation *sae2* mutant plasmids (2 μ). (F) Summary of Sae2 self-interaction domains. Two separate regions are required for the interaction between Sae2, a region containing L25 (domain A, light shading), and a region between 120 and 170 aa (domain B, dark shading). Asterisks (*) indicate antibody heavy and light chains. Double asterisks (**) indicate nonspecific signal.

To determine whether this interaction remains intact in *sae2* mutants, we performed co-IP experiments in diploid strains carrying integrated *SAE2-HA* and *FLAG-sae2* mutants. As shown in Figure 6B, among the full-

length *sae2* mutants, only *sae2-58* did not coprecipitate with Sae2-HA (lane 10). *sae2-58* is null for all phenotypes that we examined (Figure 3 and Table 1), indicating that Sae2-Sae2 interaction is required for its function. The

sae2-12 protein, a C-terminal truncation mutant, coprecipitated with Sae2-HA (Figure 6B, lane 9), indicating that the interaction domain is located in the N-terminal region. *sae2-58* contains two mutations in the N-terminal half, *L25P* and *E171G*. As shown in Figure 6C, we found that the region encompassing residue L25 is required for the interaction, since Sae2-HA IP pulled down *sae2-E171G* (lanes 5 and 6), but not *sae2-L25P* (lanes 7 and 8). Consistently, overexpression of *sae2-L25P* behaved as *sae2-58*, and *sae2-E171G* as wild type in the MMS sensitivity of *rad50S mec1* (Figure 6D).

To further test the N-terminal domain of Sae2 in the self-interaction, we generated three N-terminal truncation mutants with a C-terminal HA tag (*sae2-ΔN₁₂₀*, *-ΔN₁₇₀*, and *-ΔN₂₂₅*). Unexpectedly, *sae2-ΔN₁₂₀*, which lost L25, pulled down wild-type Sae2 and *sae2-12* (lanes 5 and 6), while *sae2-ΔN₁₇₀* did not (lanes 7 and 8), demonstrating that the additional region between residues 120 and 170 is required for the interaction (Figure 6E). *sae2-ΔN₂₂₅* may be misfolded as HA antibody did not pull down this protein. We concluded that Sae2 oligomerization via two domains in the N-terminal half is required for DNA repair, meiosis, and checkpoint functions.

DISCUSSION

The genetic relationship between Sae2 and the Mre11 complex suggests that Sae2 may antagonize checkpoint regulation, while, on the other hand, enhancing Mre11 nuclease functions. In this study, we find evidence that the association of the Mre11 complex with DSB ends may be influenced by Sae2, but this does not appear to be the basis of the Sae2 effect on checkpoint signaling. The *sae2* mutant panel confirms the influence on the DNA repair functions of the Mre11 complex and contains separation-of-function alleles that parse the influence on the Mre11 nuclease in substrate-specific manner. Finally, the data demonstrate that Sae2 self-interaction and oligomerization are critical to its function.

Specificity of Sae2 regulation of the Mre11 complex nuclease function: As summarized in Table 1, we observed a consistent correlation between *sae2* phenotypes in CPT sensitivity and the defects in processing of Spo11-DNA intermediates. Both these contexts presumably require the cleavage of DNA with protein covalently attached to it, suggesting that the Mre11-complex-dependent aspects of such cleavage events are strictly dependent upon Sae2. Alleles in this class are also synthetically lethal with Rad27 deficiency, further suggesting that the impairment of Mre11 nuclease function engendered by these *sae2* alleles exacerbates the effects of DNA lesions stabilized by the absence of Rad27.

The *sae2-51* allele (*E24V*) suggests that the influence of Sae2 on Mre11-complex-dependent hairpin cleavage may be mechanistically distinct. This allele exhibited severe defects in hairpin DNA repair, whereas it was

proficient for other functions and did not exhibit MMS and CPT sensitivity, defects in Spo11 cleavage, or synthetic lethality with *rad27Δ* (Table 1, Figure 3, and supplemental Figure S2 and Table S1 at <http://www.genetics.org/supplemental/>). On the basis of a recent report on biochemical functions of Sae2 (LENGSFELD *et al.* 2007), endonuclease activity appears to be present at the C terminus. However, it did not rule out the possibility that the N terminus of Sae2 may also have hairpin processing activity, as the N-terminal truncation lost the ability to bind DNA. Therefore, it is possible that the N terminus of Sae2 may directly be required for cleavage of hairpin DNA or may specifically regulate Mre11-complex nuclease activity on hairpins. Further investigation of *sae2-51* allele, in particular with respect to the disposition of E24 in the higher-order Sae2 structure and nuclease activity, will provide important insight regarding the biochemical functions of Sae2.

Despite failing to inhibit the TM pathway when overexpressed, the *sae2-1* allele appeared to be wild type for most phenotypes (Figure 3 and Table 1). *sae2-1* was not sensitive to CPT; however, *sae2-1* suppressed the CPT sensitivity of a *mec1Δ* mutant, while *sae2Δ* and the remaining *sae2* alleles were unable to suppress (Figure 3B). These results suggest that Mec1 influences Sae2 function, consistent with previous data demonstrating that it is a Mec1/Tel1 substrate (BARONI *et al.* 2004).

The only region of Sae2 that exhibits any conservation is at the C terminus (Figure 7A). This region appears to be required for Spo11 cleavage, as the overexpression of *sae2-ΔN₁₂₀* or *sae2-ΔN₁₇₀* could support sporulation in *sae2Δ* cells, whereas the overexpression of *sae2-12* (ΔC_{170}) could not (supplemental Table S1). In addition, overexpression of *sae2-58* could partially suppress MMS sensitivity of *sae2Δ*, whereas *sae2-ΔN₁₇₀* could not (supplemental Table S1 and Figure S3). These observations indicate that sporulation and DNA repair are mechanically distinctive.

Role of Sae2 in TM pathway: The genetic interaction between *SAE2* and the Mre11 complex strongly suggests that they may physically interact. We can reproducibly co-immunoprecipitate Sae2 with components of the Mre11 complex, but this apparent interaction requires the presence of DNA (data not shown). Interestingly, upon cell fractionation, the majority of Sae2 was found associated with chromatin; hence, it remains a possibility that Sae2 and the Mre11 complex physically associate on chromatin.

Mre11 associates more efficiently with DSB sites in the absence of Sae2 (Figure 5), perhaps suggesting that the role of Sae2 may be to inhibit Mre11-chromatin association. Although GFP fusions of Sae2 were shown to form foci in response to ionizing radiation (LISBY *et al.* 2004), we did not detect Sae2-DSB association even when *SAE2* was overexpressed (data not shown). In light of these observations, it would seem parsimonious to conclude that Sae2 does not inhibit Mre11-complex-

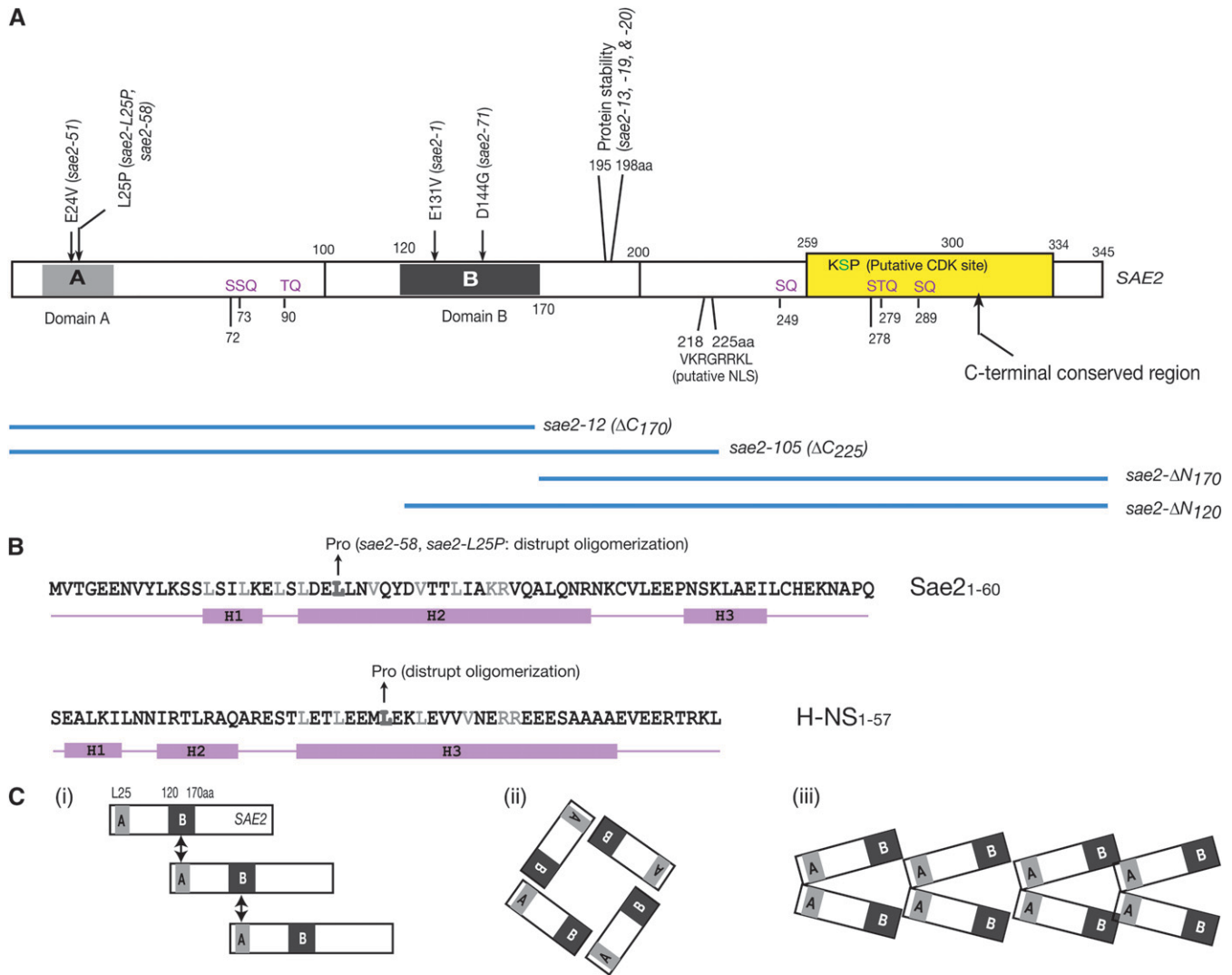


FIGURE 7.—(A) Schematic of Sae2 and *sae2* mutants. The sites of mutations in *sae2* alleles and interaction domains (domains A and B) are illustrated. The yellow box indicates the region conserved among 10 fungal species, including *Saccharomyces cerevisiae*, *Ashbya gossypii*, *Aspergillus nidulans*, *Candida glabrata*, *Debaryomyces hansenii*, *Fusarium graminearum*, *Kluyveromyces lactis*, *Magnaporthe grisea*, *Neurospora crassa*, and *Yarrowia lipolytica*. Mec1/Tel1-phosphorylation sites (SQ/TQ motif) are written in purple and the putative CDK phosphorylation (KSP) site in green in the yellow box. Truncation mutants are illustrated with blue bars. Putative nuclear localization signal (NLS). (B) Comparison between the N-terminal regions of Sae2 and H-NS. The N-terminal region of Sae2 is predicted to have three helices and this region may provide an interaction interface via the leucine-zipper structure. The similarity of secondary structure between the N terminus of Sae2 and bacterial protein H-NS is illustrated. Impairment of oligomerization by Leu-to-Pro mutation, together with the predicted secondary structure of the Sae2 N-terminal region, supports a possibility of coiled-coil interaction for Sae2 oligomerization. (C) Three different scenarios of Sae2 higher-order structure formation: (i) Sae2 may form an elongated filament-like structure via the interaction between domains A and B; (ii) Sae2 may form rather defined structure, for example, tetramers; the interaction between domains A and B may determine the shape and size of multimers; and (iii) Sae2 may dimerize first and then assemble to form a filament-like higher-order structure.

dependent signaling by inhibiting DNA damage recognition; however, our data do not strictly rule out a kinetic effect of Sae2 on Mre11 complex dynamics at DSBs.

Higher-order structure of Sae2: Sae2 has two interaction domains in the N-terminal half, a region around L25 (domain A) and a region between 120 and 170 amino acids (domain B). Co-immunoprecipitation data (Figure 6) indicates that interaction appears to occur via domain A and B, and A and A, but not B and B, as *sae2-*

L25P lost the ability to associate with wild-type Sae2. This suggests several modes of interaction that could be organized to form oligomeric structures pictured in Figure 7C.

We favor the idea that Sae2 multimerizes as opposed to simple dimerization. The affect of overexpressing *sae2* mutations in *rad50S mec1Δ* cells is influenced by the presence of a wild-type *SAE2* gene on the chromosome. For example, the rescue of *mec1Δ* MMS sensitivity by *rad50S* was not inhibited by *sae2-1* overexpression

(Figure 2A); hence, even though *sae2-1* is present in at least 5- to 10-fold excess, wild-type Sae2 protein exerts a significant effect. In contrast, overexpressing *sae2-1* with no wild-type Sae2 present abrogated the suppressive effect of *sae2Δ* on *mec1Δ* (supplemental Figure S1), suggesting that overproduced *sae2-1* protein may be able to form partially functional homomultimers. Overexpression of seven of the *sae2* mutants (*sae2-51*, *-71*, *-78*, *-97*, *-102*, *-110*, and *-142*) showed similar phenotypes to *sae2-1* overexpression (supplemental Table S1 and Figure S1). Five of these alleles (*sae2-1*, *-51*, *-71*, *-110*, and *-142*) have mutations in one of the interaction domains. Sae2–Sae2 self-association, however, appears to be intact in all of these *sae2* mutants. These features are similar to some of the dominant-negative p53 mutants that interact with wild-type p53, resulting in dysfunctional tetramer formation (MILNER and MEDCALF 1991; SUN *et al.* 1993; WANG *et al.* 1994).

Alternatively, Sae2 may dimerize first and then self-assemble to form higher-order structure (Figure 7C, iii), similar to H-NS, a nucleoid-associated protein in bacteria (DORMAN 2004). H-NS contains an N-terminal oligomerization domain (BLOCH *et al.* 2003), and structural- and microscopy-based studies have shown that a coiled-coil interaction between helix H3 (rich in Leu and Val) of two H-NS proteins mediates the dimerization (UEGUCHI *et al.* 1996; DAME *et al.* 2000; ESPOSITO *et al.* 2002; BLOCH *et al.* 2003). Head-to-tail assembly of the dimers then forms a filament-like, higher-order structure. The mutation of Leu29 to proline, a helix breaker, results in the inability of H-NS to oligomerize, presumably by preventing formation of the initial dimers (UEGUCHI *et al.* 1997). As illustrated in Figure 7B, residues 1–60 of the Sae2 N terminus are predicted to form three helices. Helix H2 consists of residues 22–45, with every 3–4 residues occupied by leucine or valine. Similar to the situation with H-NS, a Sae2 *L25P* mutation abolished the oligomerization of Sae2 (Figure 6C); in addition, overexpression of the H-NS oligomerization domain exhibited dominant-negative effects (WILLIAMS *et al.* 1996; UEGUCHI *et al.* 1997), similar to some of our *sae2* mutant alleles. Interestingly, however, an *E24V* mutation did not disrupt the Sae2 self-interaction, further supporting the idea that the N terminus of Sae2 may form a hydrophobic interaction surface, similar to H-NS.

A putative *SAE2* homolog, CtIP, has recently been identified in humans, worms, and plants (PENKNER *et al.* 2007; SARTORI *et al.* 2007; UANSCHOU *et al.* 2007). CtIP has sequence homology to budding yeast *SAE2* at the C-terminal region, a small domain that is conserved in several fungal species. Similar to *sae2Δ*, CtIP deficiency is associated with defects in processing of meiotic DSBs, and evidence for alteration in the processing of mitotic DSBs has been presented and CtIP appears to be required for recruitment of ATR in human cells (SARTORI *et al.* 2007). The data presented here shed light on Sae2's mechanisms of action and illustrate that its in-

fluence on nuclease activities required for DSB metabolism varies according to the substrate, as well as the status of the checkpoint pathway.

We thank Maria Pia Longhese for the *SAE2-HA* strain and Michael Lichten for yeast strains for chromatin immunoprecipitation experiments; Gene Bryant and Daniel Spagna in the Mark Ptashne lab for technical help for real-time PCR; and the members of our labs for insightful discussion over the course of this work. This work was supported by grants GM56888 and GM59413 and the Joel and Joan Smilow Initiative (J.H.J.P.), grant GM61766 (J.E.H.) and National Science Foundation MCB-0344655, and Binational Agriculture Research and Development award IS-372305 (C.W.).

LITERATURE CITED

- BARONI, E., V. VISCARDI, H. CARTAGENA-LIROLA, G. LUCCHINI and M. P. LONGHESE, 2004 The functions of budding yeast Sae2 in the DNA damage response require Mec1- and Tel1-dependent phosphorylation. *Mol. Cell Biol.* **24**: 4151–4165.
- BLOCH, V., Y. YANG, E. MARGEAT, A. CHAVANIEU, M. T. AUGE *et al.*, 2003 The H-NS dimerization domain defines a new fold contributing to DNA recognition. *Nat. Struct. Biol.* **10**: 212–218.
- BORDE, V., W. LIN, E. NOVIKOV, J. H. PETRINI, M. LICHTEN *et al.*, 2004 Association of Mre11p with double-strand break sites during yeast meiosis. *Mol. Cell* **13**: 389–401.
- CAO, L., E. ALANI and N. KLECKNER, 1990 A pathway for generation and processing of double-strand breaks during meiotic recombination in *S. cerevisiae*. *Cell* **61**: 1089–1101.
- CLERICI, M., D. MANTIERO, G. LUCCHINI and M. P. LONGHESE, 2006 The *Saccharomyces cerevisiae* Sae2 protein negatively regulates DNA damage checkpoint signalling. *EMBO Rep.* **7**: 212–218.
- D'ADDA DI FAGAGNA, F., P. M. REAPER, L. CLAY-FARRACE, H. FIEGLER, P. CARR *et al.*, 2003 A DNA damage checkpoint response in telomere-initiated senescence. *Nature* **426**: 194–198.
- DAME, R. T., C. WYMAN and N. GOOSEN, 2000 H-NS mediated compaction of DNA visualised by atomic force microscopy. *Nucleic Acids Res.* **28**: 3504–3510.
- D'AMOURS, D., and S. P. JACKSON, 2002 The Mre11 complex: at the crossroads of DNA repair and checkpoint signalling. *Nat. Rev. Mol. Cell Biol.* **3**: 317–327.
- DEBRAUWERE, H., S. LOEILLET, W. LIN, J. LOPES and A. NICOLAS, 2001 Links between replication and recombination in *Saccharomyces cerevisiae*: a hypersensitive requirement for homologous recombination in the absence of Rad27 activity. *Proc. Natl. Acad. Sci. USA* **98**: 8263–8269.
- DENG, C., J. A. BROWN, D. YOU and J. M. BROWN, 2005 Multiple endonucleases function to repair covalent topoisomerase I complexes in *Saccharomyces cerevisiae*. *Genetics* **170**: 591–600.
- DORMAN, C. J., 2004 H-NS: a universal regulator for a dynamic genome. *Nat. Rev. Microbiol.* **2**: 391–400.
- ESPOSITO, D., A. PETROVIC, R. HARRIS, S. ONO, J. F. ECCLESTON *et al.*, 2002 H-NS oligomerization domain structure reveals the mechanism for high order self-association of the intact protein. *J. Mol. Biol.* **324**: 841–850.
- ITO, T., T. CHIBA, R. OZAWA, M. YOSHIDA, M. HATTORI *et al.*, 2001 A comprehensive two-hybrid analysis to explore the yeast protein interactome. *Proc. Natl. Acad. Sci. USA* **98**: 4569–4574.
- KEENEY, S., and N. KLECKNER, 1995 Covalent protein-DNA complexes at the 5' strand termini of meiosis-specific double-strand breaks in yeast. *Proc. Natl. Acad. Sci. USA* **92**: 11274–11278.
- KEENEY, S., C. N. GIROUX and N. KLECKNER, 1997 Meiosis-specific DNA double-strand breaks are catalyzed by Spo11, a member of a widely conserved protein family. *Cell* **88**: 375–384.
- KIRONMAI, K. M., and K. MUNIYAPPA, 1997 Alteration of telomeric sequences and senescence caused by mutations in RAD50 of *Saccharomyces cerevisiae*. *Genes Cells* **2**: 443–455.
- LEE, S. E., J. K. MOORE, A. HOLMES, K. UMEZU, R. D. KOLODNER *et al.*, 1998 *Saccharomyces* Ku70, Mre11/Rad50, and RPA proteins regulate adaptation to G2/M arrest after DNA damage. *Cell* **94**: 399–409.

- LEE, S. E., D. A. BRESSAN, J. H. J. PETRINI and J. E. HABER, 2002 Complementation between N-terminal *Saccharomyces cerevisiae mre11* alleles in DNA repair and telomere length maintenance. *DNA Repair* **1**: 27–40.
- LENGSFELD, B. M., A. J. RATTRAY, V. BHASKARA, R. GHIRLANDO and T. T. PAULL, 2007 Sae2 Is an endonuclease that processes hairpin DNA cooperatively with the Mre11/Rad50/Xrs2 complex. *Mol. Cell* **28**: 638–651.
- LEROY, C., S. E. LEE, M. B. VAZE, F. OCHSENBIEN, R. GUEROIS *et al.*, 2003 PP2C phosphatases Ptc2 and Ptc3 are required for DNA checkpoint inactivation after a double-strand break. *Mol. Cell* **11**: 827–835.
- LISBY, M., J. H. BARLOW, R. C. BURGESS and R. ROTHSTEIN, 2004 Choreography of the DNA damage response: spatiotemporal relationships among checkpoint and repair proteins. *Cell* **118**: 699–713.
- LOBACHEV, K. S., D. A. GORDENIN and M. A. RESNICK, 2002 The Mre11 complex is required for repair of hairpin-capped double-strand breaks and prevention of chromosome rearrangements. *Cell* **108**: 183–193.
- LUNDBLAD, V., 2002 Telomere maintenance without telomerase. *Oncogene* **21**: 522–531.
- McKEE, A. H., and N. KLECKNER, 1997 A general method for identifying recessive diploid-specific mutations in *Saccharomyces cerevisiae*, its application to the isolation of mutants blocked at intermediate stages of meiotic prophase and characterization of a new gene *SAE2*. *Genetics* **146**: 797–816.
- MILNER, J., and E. A. MEDCALF, 1991 Cotranslation of activated mutant p53 with wild type drives the wild-type p53 protein into the mutant conformation. *Cell* **65**: 765–774.
- MORALES, M., J. W. THEUNISSEN, C. F. KIM, R. KITAGAWA, M. B. KASTAN *et al.*, 2005 The Rad50S allele promotes ATM-dependent DNA damage responses and suppresses ATM deficiency: implications for the Mre11 complex as a DNA damage sensor. *Genes Dev.* **19**: 3043–3054.
- MOREAU, S., J. R. FERGUSON and L. S. SYMINGTON, 1999 The nuclease activity of Mre11 is required for meiosis but not for mating type switching, end joining, or telomere maintenance. *Mol. Cell Biol.* **19**: 556–566.
- MOREAU, S., E. A. MORGAN and L. S. SYMINGTON, 2001 Overlapping functions of the *Saccharomyces cerevisiae* Mre11, Exo1 and Rad27 nucleases in DNA metabolism. *Genetics* **159**: 1423–1433.
- NAIRZ, K., and F. KLEIN, 1997 mre11S: a yeast mutation that blocks double-strand-break processing and permits nonhomologous synapsis in meiosis. *Genes Dev.* **11**: 2272–2290.
- PANDITA, T. K., 2002 ATM function and telomere stability. *Oncogene* **21**: 611–618.
- PELLICCIOLI, A., S. E. LEE, C. LUCCA, M. FOIANI and J. E. HABER, 2001 Regulation of *Saccharomyces* Rad53 checkpoint kinase during adaptation from DNA damage-induced G2/M arrest. *Mol. Cell* **7**: 293–300.
- PENKNER, A., Z. PORTIK-DOBOS, L. TANG, R. SCHNABEL, M. NOVATCHKOVA *et al.*, 2007 A conserved function for a *Caenorhabditis elegans* Com1/Sae2/CtIP protein homolog in meiotic recombination. *EMBO J.* **26**: 5071–5082.
- PETRINI, J. H., and T. H. STRACKER, 2003 The cellular response to DNA double-strand breaks: defining the sensors and mediators. *Trends Cell Biol.* **13**: 458–462.
- PRINZ, S., A. AMON and F. KLEIN, 1997 Isolation of COM1, a new gene required to complete meiotic double-strand break-induced recombination in *Saccharomyces cerevisiae*. *Genetics* **146**: 781–795.
- RATTRAY, A. J., C. B. MCGILL, B. K. SHAFER and J. N. STRATHERN, 2001 Fidelity of mitotic double-strand-break repair in *Saccharomyces cerevisiae*: a role for *SAE2/COM1*. *Genetics* **158**: 109–122.
- RITCHIE, K. B., and T. D. PETES, 2000 The Mre11p/Rad50p/Xrs2p complex and the Tel1p function in a single pathway for telomere maintenance in yeast. *Genetics* **155**: 475–479.
- SARTORI, A. A., C. LUKAS, J. COATES, M. MISTRIK, S. FU *et al.*, 2007 Human CtIP promotes DNA end resection. *Nature* **450**: 509–514.
- SHIMA, H., M. SUZUKI and M. SHINOHARA, 2005 Isolation and characterization of novel xrs2 mutations in *Saccharomyces cerevisiae*. *Genetics* **170**: 71–85.
- SHROFF, R., A. ARBEL-EDEN, D. PILCH, G. IRA, W. M. BONNER *et al.*, 2004 Distribution and dynamics of chromatin modification induced by a defined DNA double-strand break. *Curr. Biol.* **14**: 1703–1711.
- STRACKER, T. H., J. W. THEUNISSEN, M. MORALES and J. H. PETRINI, 2004 The Mre11 complex and the metabolism of chromosome breaks: the importance of communicating and holding things together. *DNA Repair (Amst.)* **3**: 845–854.
- SUN, Y., Z. DONG, K. NAKAMURA and N. H. COLBURN, 1993 Dosage-dependent dominance over wild-type p53 of a mutant p53 isolated from nasopharyngeal carcinoma. *FASEB J.* **7**: 944–950.
- UANSCHOU, C., T. SIWIEC, A. PEDROSA-HARAND, C. KERZENDORFER, E. SANCHEZ-MORAN *et al.*, 2007 A novel plant gene essential for meiosis is related to the human CtIP and the yeast COM1/SAE2 gene. *EMBO J.* **26**: 5061–5070.
- UEGUCHI, C., T. SUZUKI, T. YOSHIDA, K. TANAKA and T. MIZUNO, 1996 Systematic mutational analysis revealing the functional domain organization of *Escherichia coli* nucleoid protein H-NS. *J. Mol. Biol.* **263**: 149–162.
- UEGUCHI, C., C. SETO, T. SUZUKI and T. MIZUNO, 1997 Clarification of the dimerization domain and its functional significance for the *Escherichia coli* nucleoid protein H-NS. *J. Mol. Biol.* **274**: 145–151.
- USUI, T., H. OGAWA and J. H. PETRINI, 2001 A DNA damage response pathway controlled by Tel1 and the Mre11 complex. *Mol. Cell* **7**: 1255–1266.
- USUI, T., J. H. PETRINI and M. MORALES, 2006 Rad50S alleles of the Mre11 complex: questions answered and questions raised. *Exp. Cell Res.* **312**: 2694–2699.
- VANCE, J. R., and T. E. WILSON, 2002 Yeast Tdp1 and Rad1-Rad10 function as redundant pathways for repairing Top1 replicative damage. *Proc. Natl. Acad. Sci. USA* **99**: 13669–13674.
- VAZE, M. B., A. PELLICCIOLI, S. E. LEE, G. IRA, G. LIBERI *et al.*, 2002 Recovery from checkpoint-mediated arrest after repair of a double-strand break requires Srs2 helicase. *Mol. Cell* **10**: 373–385.
- WANG, P., M. REED, Y. WANG, G. MAYR, J. E. STENGER *et al.*, 1994 p53 domains: structure, oligomerization, and transformation. *Mol. Cell Biol.* **14**: 5182–5191.
- WEIL, C. F., and R. KUNZE, 2000 Transposition of maize Ac/Ds transposable elements in the yeast *Saccharomyces cerevisiae*. *Nat. Genet.* **26**: 187–190.
- WILLIAMS, R. M., S. RIMSKY and H. BUC, 1996 Probing the structure, function, and interactions of the *Escherichia coli* H-NS and StpA proteins by using dominant negative derivatives. *J. Bacteriol.* **178**: 4335–4343.
- YU, J., K. MARSHALL, M. YAMAGUCHI, J. E. HABER and C. F. WEIL, 2004 Microhomology-dependent end joining and repair of transposon-induced DNA hairpins by host factors in *Saccharomyces cerevisiae*. *Mol. Cell Biol.* **24**: 1351–1364.
- ZHOU, B. B., and S. J. ELLEDGE, 2000 The DNA damage response: putting checkpoints in perspective. *Nature* **408**: 433–439.